Mechanics of noncoplanar mesh design for stretchable electronic circuits

J. Song,[1,a)] Y. Huang,[2,3] J. Xiao,[3] S. Wang,[3] K. C. Hwang,[4] H. C. Ko,[5] D.-H. Kim,[5] M. P. Stoykovich,[6] and J. A. Rogers[5,7,b)]
[1]*Department of Mechanical and Aerospace Engineering, University of Miami, Coral Gables, Florida 33146, USA*
[2]*Department of Civil and Environmental Engineering, Northwestern University, Evanston, Illinois 60208, USA*
[3]*Department of Mechanical Engineering, Northwestern University, Evanston, Illinois 60208, USA*
[4]*Department of Engineering Mechanics, Tsinghua University, Beijing 100084, China*
[5]*Department of Materials Science and Engineering, University of Illinois, Urbana, Illinois 61801, USA*
[6]*Department of Chemical and Biological Engineering, University of Colorado, Boulder, Colorado 80309, USA*
[7]*Department of Mechanical Science and Engineering, Department of Electrical and Computer Engineering, Department of Chemistry, and Frederick Seitz Materials Research Laboratory, University of Illinois, Urbana, Illinois 61801, USA*

(Received 17 February 2009; accepted 7 May 2009; published online 22 June 2009)

A noncoplanar mesh design that enables electronic systems to achieve large, reversible levels stretchability (>100%) is studied theoretically and experimentally. The design uses semiconductor device islands and buckled thin interconnects on elastometric substrates. A mechanics model is established to understand the underlying physics and to guide the design of such systems. The predicted buckle amplitude agrees well with experiments within 5.5% error without any parameter fitting. The results also give the maximum strains in the interconnects and the islands, as well as the overall system stretchability and compressibility. © *2009 American Institute of Physics*.
[DOI: 10.1063/1.3148245]

I. INTRODUCTION

Stretchable electronics is emerging as a technology that could be valuable for various applications such as flexible displays,[1] electronic eye camera,[2] conformable skin sensors,[3] smart surgical gloves,[4] and structural health monitoring devices.[5] There exist two approaches to achieve stretchability: (i) coplanar stretchable interconnects (bonded to a substrate) between rigid device islands,[6] and (ii) wavy layout (i.e., small wave) throughout the whole circuit system.[7] Both are fabricated on elastometric substrates, and provide some degree of stretchability (e.g., 10%). None offers strain-independent electronic performance at large strains, which is of interest in practical applications.[2,4] Here, we present a noncoplanar mesh design, which is based on the interconnect-island[6] concept to accomplish much higher stretchability (i.e., up to 100%). Figure 1 schematically illustrates the fabrication of circuits with noncoplanar mesh design on compliant substrates.[2,8] The silicon (or other semiconductor material) islands, on which the active devices or circuits are fabricated, are chemically bonded to a prestrained (e.g., 50%) elastometric substrate of a material such as poly(dimethylsiloxane) (PDMS), while interconnects are loosely bonded.[8] Releasing the prestrain leads to compression, which causes the interconnects to buckle and move out of the plane of the substrate to form arc-shaped structures. The poor adhesion of interconnects (to PDMS) and their narrow geometries and low stiffness (compared to device islands) cause the out-of-plane deformation to localize only to interconnects, and therefore the strain in islands is very small. Figure 2 shows a scanning electron micrograph of silicon structure (island: 20×20 μm^2, 50 nm thick; interconnect: 20×4 μm^2, 50 nm thick) on a 1 mm thick PDMS substrate. The inset clearly shows that the islands remain flat while interconnects buckle.

Kim *et al.*[8] developed a full-scale finite element model for the noncoplanar mesh design. But, it is rather complex and does not lead to simple, analytical solutions to be used in the design and optimization of these systems. This paper

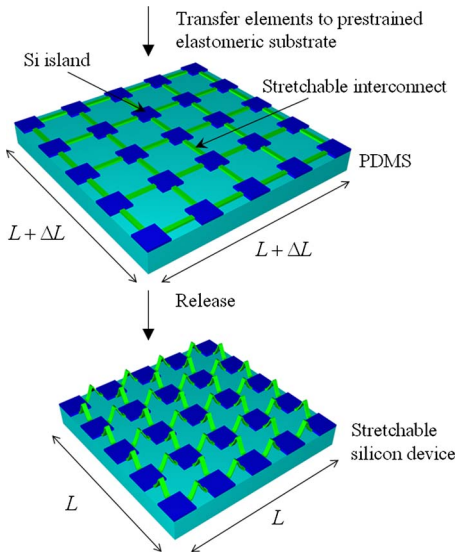

FIG. 1. (Color online) Schematic illustration of the process for fabricating electronics with noncoplanar mesh designs on a complaint substrate.

[a)]Author to whom correspondence should be addressed. Electronic mail: jsong8@miami.edu.
[b)]Electronic mail: jrogers@uiuc.edu.

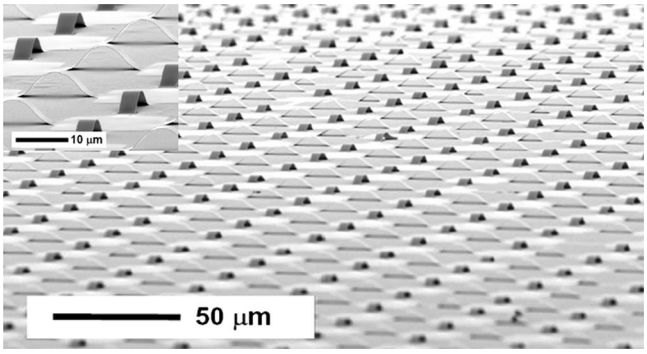

FIG. 2. A scanning electron micrograph of a noncoplanar silicon mesh structure (island: 20×20 μm^2, 50 nm thick; interconnect: 20×4 μm^2, 50 nm thick) on a PDMS substrate.

aims at establishing a mechanics theory for the mechanical response of noncoplanar mesh design and predicting the maximum strains in the interconnects as well as in the islands, which are both important to determine the stretchability of the system. For simplicity, silicon is used for both islands and interconnects, though the mechanics theory can be applied to other systems that involve multiple materials. The paper is outlined as follows. The mechanics models of the interconnects and the islands are described in Secs. II and III, respectively. Stretchability/compressibility of various nonplanar mesh designs are discussed in Sec. IV.

II. MECHANICS MODEL OF INTERCONNECTS

The width of interconnects is much smaller than the width of island such that the rotation at the ends of interconnects is very small. This is verified by the finite element analysis (see Sec. III and also Kim *et al.*[8]) as well as by the analytical solution given in the Appendix. Therefore, the "bridge"-like interconnect is modeled as a beam with clamped ends (as shown in Fig. 3) since its thickness ($h_{\text{bridge}}\sim50$ nm) is much smaller than any other characteristic length (width: $w_{\text{bridge}}\sim4$ μm; length: $L_{\text{bridge}}\sim20$ μm). The beam, however, undergoes large rotation once the interconnect buckles. Let X denote the initial, strain-free configuration of the beam (top figure in Fig. 1), and x the buckled configuration (bottom figure in Fig. 1). The distance between islands changes from L^0_{bridge} to L_{bridge} in these two configurations, as shown in Fig. 3, and the buckle amplitude A is to be determined. The out-of-plane displacement w of the interconnect takes the form

$$w=\frac{A}{2}\left(1+\cos\frac{2\pi x}{L_{\text{bridge}}}\right)=\frac{A}{2}\left(1+\cos\frac{2\pi X}{L^0_{\text{bridge}}}\right), \tag{1}$$

which satisfies vanishing displacement and slope at the two ends $X=\pm L^0_{\text{bridge}}/2$. The sinusoidal buckle profile in the

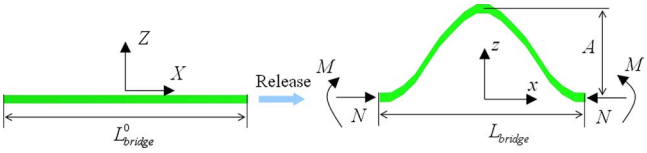

FIG. 3. (Color online) Schematic diagram of mechanics model for the interconnect region of a noncoplanar mesh structure.

above equation also agrees well with the full-scale finite element analysis.[8]

The total energy $U^{\text{tot}}_{\text{bridge}}$ of the interconnect consists the bending energy $U^{\text{bending}}_{\text{bridge}}$ and the membrane energy $U^{\text{membrane}}_{\text{bridge}}$. The bending energy $U^{\text{bending}}_{\text{bridge}}$ can be obtained from Eq. (1) and the bending rigidity $E_{\text{bridge}}h^3_{\text{bridge}}/12$ as

$$U^{\text{bending}}_{\text{bridge}}=\int_{-L^0_{\text{bridge}}/2}^{L^0_{\text{bridge}}/2}\frac{1}{2}\frac{E_{\text{bridge}}h^3_{\text{bridge}}}{12}\left(\frac{d^2w}{dX^2}\right)^2dX$$

$$=\frac{E_{\text{bridge}}h^3_{\text{bridge}}}{12}\frac{\pi^4A^2}{(L^0_{\text{bridge}})^3}, \tag{2}$$

where E_{bridge} is the Young's modulus of the interconnect.

The membrane strain $\varepsilon^{\text{membrane}}_{\text{bridge}}$, which determines the membrane energy, is related to the out-of-plane displacement w in Eq. (1) and in-plane displacement u by[9]

$$\varepsilon^{\text{membrane}}_{\text{bridge}}=\frac{du}{dX}+\frac{1}{2}\left(\frac{dw}{dX}\right)^2. \tag{3}$$

The membrane force N is then related to $\varepsilon^{\text{membrane}}_{\text{bridge}}$ via the tension rigidity $E_{\text{bridge}}h_{\text{bridge}}$ as $N=E_{\text{bridge}}h_{\text{bridge}}\varepsilon^{\text{membrane}}_{\text{bridge}}$. The force equilibrium

$$\frac{dN}{dX}=0, \tag{4}$$

requires a constant membrane force, which gives the in-plane displacement

$$u=\left(\frac{\pi A^2}{16L^0_{\text{bridge}}}\right)\sin\left(\frac{4\pi}{L^0_{\text{bridge}}}X\right)-\frac{L^0_{\text{bridge}}-L_{\text{bridge}}}{L^0_{\text{bridge}}}X. \tag{5}$$

Here the conditions $u(0)=0$ and $\int_{-L^0_{\text{bridge}}/2}^{L^0_{\text{bridge}}/2}du=L_{\text{bridge}}-L^0_{\text{bridge}}$ have been imposed. Equation (3) then gives a constant membrane strain

$$\varepsilon^{\text{membrane}}_{\text{bridge}}=\frac{\pi^2A^2}{4(L^0_{\text{bridge}})^2}-\frac{L^0_{\text{bridge}}-L_{\text{bridge}}}{L^0_{\text{bridge}}}. \tag{6}$$

The membrane energy in the interconnect is given by

$$U^{\text{membrane}}_{\text{bridge}}=\int_{-L^0_{\text{bridge}}/2}^{L^0_{\text{bridge}}/2}\frac{1}{2}E_{\text{bridge}}h_{\text{bridge}}(\varepsilon^{\text{membrane}}_{\text{bridge}})^2dX$$

$$=\frac{1}{2}E_{\text{bridge}}h_{\text{bridge}}L^0_{\text{bridge}}\left[\frac{\pi^2A^2}{4(L^0_{\text{bridge}})^2}+\frac{L_{\text{bridge}}-L^0_{\text{bridge}}}{L^0_{\text{bridge}}}\right]^2. \tag{7}$$

Minimization of total energy in the interconnect $\partial U^{\text{tot}}_{\text{bridge}}/\partial A=0$ gives the amplitude

$$A=\frac{2L^0_{\text{bridge}}}{\pi}\sqrt{\frac{L^0_{\text{bridge}}-L_{\text{bridge}}}{L^0_{\text{bridge}}}-\varepsilon_c}, \tag{8}$$

where $\varepsilon_c=\pi^2h^2_{\text{bridge}}/[3(L^0_{\text{bridge}})^2]$ is the critical buckling strain for Euler buckling of a doubly clamped beam. For $(L^0_{\text{bridge}}-L_{\text{bridge}})/L^0_{\text{bridge}}<\varepsilon_c$, the interconnect does not buckle, and therefore has no bending. The membrane strain is $\varepsilon^{\text{membrane}}_{\text{bridge}}=-(L^0_{\text{bridge}}-L_{\text{bridge}})/L^0_{\text{bridge}}$. Once $(L^0_{\text{bridge}}-L_{\text{bridge}})/L^0_{\text{bridge}}$ exceeds ε_c, the interconnect buckles such that the membrane

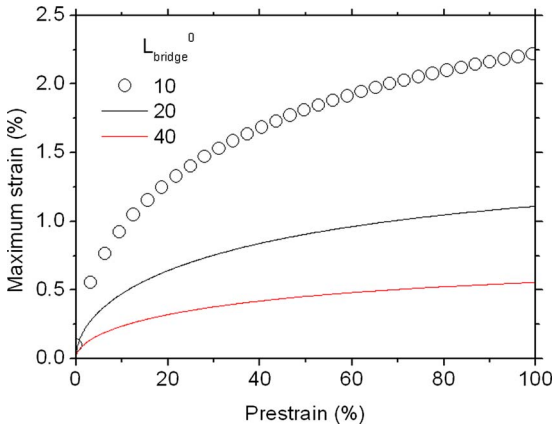

FIG. 4. (Color online) The maximum strain in the interconnects vs the prestrain for different interconnect lengths.

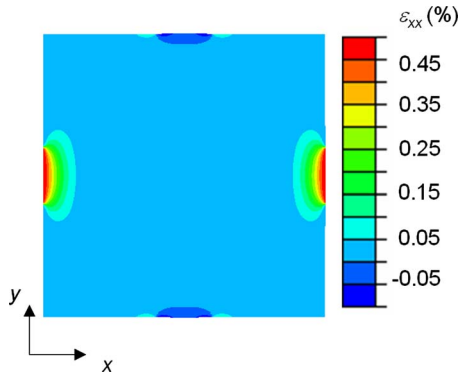

FIG. 5. (Color online) Distribution of the strain ε_{xx} in islands (20×20 μm^2) when the interconnect relaxes from 20 to 17.5 μm.

strain remains a constant $-\varepsilon_c$ [see from Eqs. (6) and (8)], and the bending strain (curvature $^* h_{bridge}/2$) increases with the deformation, $\varepsilon_{bridge}^{bending} = 2\pi(h_{bridge}/L_{bridge}^0) \times \sqrt{[(L_{bridge}^0 - L_{bridge})/L_{bridge}^0]} - \varepsilon_c$. The maximum (compressive) strain in the interconnect is the sum of membrane and bending strains, and is given by

$$\varepsilon_{bridge}^{max} = 2\pi \frac{h_{bridge}}{L_{bridge}^0} \sqrt{\frac{L_{bridge}^0 - L_{bridge}}{L_{bridge}^0}} - \varepsilon_c + \varepsilon_c$$
$$\approx 2\pi \frac{h_{bridge}}{L_{bridge}^0} \sqrt{\frac{L_{bridge}^0 - L_{bridge}}{L_{bridge}^0}}, \quad (9)$$

where the approximation holds for $(L_{bridge}^0 - L_{bridge})/L_{bridge}^0 \gg h_{bridge}^2/(L_{bridge}^0)^2$.

Once the prestrain ε_{pre} in the substrate is relaxed, the bridge length is reduced to L_{bridge}. Therefore the prestrain is given by $\varepsilon_{pre} = (L_{bridge}^0 - L_{bridge})/L_{bridge}$, which can be rewritten as

$$\frac{L_{bridge}^0 - L_{bridge}}{L_{bridge}^0} = \frac{\varepsilon_{pre}}{1 + \varepsilon_{pre}}. \quad (10)$$

The maximum strain in the interconnect in Eq. (9) is then related to the prestrain in the substrate by

$$\varepsilon_{bridge}^{max} = 2\pi \frac{h_{bridge}}{L_{bridge}^0} \sqrt{\frac{\varepsilon_{pre}}{1 + \varepsilon_{pre}}}. \quad (11)$$

The initial length of the interconnect in experiments is $L_{bridge}^0 = 20$ μm and the thickness $h_{bridge} = 50$ nm, which give a critical buckling strain $\varepsilon_c = 0.0021\%$. The measured bridge length is $L_{bridge} = 17.5$ μm after relaxation, which corresponds to prestrain $\varepsilon_{pre} = 14.3\%$ in the substrate. Equation (8) then predicts the amplitude $A = 4.50$ μm, which agrees well with the experimentally measured amplitude 4.76 μm. The maximum strain in the interconnect is 0.56%. This value is smaller than the fracture strain of silicon (~1%), and is much smaller than the prestrain ε_{pre}. For 1% interconnect strain, the prestrain can reach 68.1%.

The maximum strain in the interconnect $\varepsilon_{bridge}^{max}$ given in Eq. (9) or Eq. (11) is proportional to the interconnect thickness and to length ratio, h_{bridge}/L_{bridge}^0. Figure 4 shows $\varepsilon_{bridge}^{max}$ versus the prestrain ε_{pre} for the length $L_{bridge}^0 = 40$, 20, and 10 μm and thickness $h_{bridge} = 50$ nm [or equivalently $h_{bridge} = 25$, 50, and 100 nm and length $L_{bridge}^0 = 20$ μm]. Therefore thin and long interconnects give small strain, and thus increase the stretchability.

III. MECHANICS MODEL OF ISLANDS

The finite element method is used to study the silicon island on PDMS substrate. The island is modeled as a plate since its thickness h_{island} is much smaller than the length L_{island}^0. The buckled interconnects give the axial force $N = E_{bridge} h_{bridge} \varepsilon_c$ and bending moment $M = (E_{bridge} h_{bridge}^3/12) \times [2\pi^2 A/(L_{bridge}^0)^2] \approx \pi E_{bridge} h_{bridge}^3/(3L_{bridge}^0)\sqrt{\varepsilon_{pre}/(1+\varepsilon_{pre})}$ over the width w_{bridge} on each edge of the island.

The PDMS substrate is modeled by a unit cell that is a square with edge length $L_{island}^0 + L_{bridge}$ in the (X-Y) plane but very thick in the island thickness direction (Z). The displacements are continuous across the island/substrate interface, and the rest of the top surface is traction free. Periodic boundary conditions are imposed on the lateral surfaces (X-Z and Y-Z planes) of the substrate.

Figure 5 shows the strain distribution ε_{xx} in a Si island ($E_{island} = 130$ GPa, $\nu_{island} = 0.27$, length $L_{island}^0 = 20$ μm, and thickness $h_{island} = 50$ nm)[10] on an PDMS substrate ($E_{substrate} = 2$ MPa and $\nu_{substrate} = 0.48$).[11] The axial force and bending moment result from the buckled interconnect ($E_{bridge} = 130$ GPa, $L_{bridge}^0 = 20$ μm, $h_{bridge} = 50$ nm, $w_{bridge} = 4$ μm, and $L_{bridge} = 17.5$ μm after relaxation). The maximum strain occurs at the interconnect/island boundary.

The strain due to the axial force is negligible as compared to that due to the bending moment. Dimensional analysis gives the maximum strain in the silicon island as $\varepsilon_{island}^{max} = \alpha 6(1 - \nu_{island}^2) M/(E_{island} h_{island}^2)$, where α is a nondimensional function of dimensionless elastic properties $E_{substrate}/E_{island}$, $\nu_{substrate}$, and ν_{island}, and nondimensional lengths w_{bridge}/L_{island} and L_{bridge}^0/L_{island}. Finite element analyses show that α is essentially a constant of unity. For large variations in island and substrate elastic properties and interconnect width w_{bridge} and length L_{bridge}^0, α only deviates from one by a few percent. The maximum strain in the silicon island is then given by

$$\varepsilon_{\text{island}}^{\max} \approx \frac{6(1-\nu_{\text{island}}^2)M}{E_{\text{island}}h_{\text{island}}^2} = 2\pi\frac{(1-\nu_{\text{island}}^2)E_{\text{bridge}}h_{\text{bridge}}^3}{E_{\text{island}}h_{\text{island}}^2 L_{\text{bridge}}^0}\sqrt{\frac{\varepsilon_{\text{pre}}}{1+\varepsilon_{\text{pre}}}}, \quad (12)$$

which can also be related to the maximum strain in interconnect by

$$\varepsilon_{\text{island}}^{\max} = \frac{(1-\nu_{\text{island}}^2)E_{\text{bridge}}h_{\text{bridge}}^2}{E_{\text{island}}h_{\text{island}}^2}\varepsilon_{\text{bridge}}^{\max}. \quad (13)$$

Therefore, a stiff and thick island reduces its strain.

The maximum prestrain $\varepsilon_{\text{pre}}^{\max}$ that the noncoplanar mesh design can accommodate is obtained by equating the strains in Eqs. (11) and (12) to the failure strains (~1%) $\varepsilon_{\text{bridge}}^{\text{failure}}$ and $\varepsilon_{\text{island}}^{\text{failure}}$ of interconnect and island materials, respectively,

$$\varepsilon_{\text{pre}}^{\max} < \frac{a^2}{1-a^2} \quad \text{if} \quad a<1, \quad (14)$$

where

$$a = \frac{L_{\text{bridge}}^0}{2\pi h_{\text{bridge}}}\min\left[\varepsilon_{\text{bridge}}^{\text{failure}}, \frac{E_{\text{island}}h_{\text{island}}^2}{(1-\nu_{\text{island}}^2)E_{\text{bridge}}h_{\text{bridge}}^2}\varepsilon_{\text{island}}^{\text{failure}}\right]. \quad (15)$$

For $a \geq 1$ (e.g., long interconnects), the maximum prestrain is then governed by the failure of PDMS substrate.

IV. STRETCHABILITY/COMPRESSIBILITY OF NONCOPLANAR MESH DESIGN

The length of a unit cell changes from $L_{\text{bridge}}^0+L_{\text{island}}^0$ to $L_{\text{bridge}}+L_{\text{island}}^0$ after the prestrain ε_{pre} is relaxed, where $L_{\text{bridge}}=L_{\text{bridge}}^0/(1+\varepsilon_{\text{pre}})$ is obtained from Eq. (10), and the change in island length is negligible because the interconnect buckles to accommodate the release of prestrain. The length of the unit cell becomes $L'_{\text{bridge}}+L_{\text{island}}^0$ once the system is subject to an applied strain $\varepsilon_{\text{applied}}$, where the length of interconnect L'_{bridge} is related to $\varepsilon_{\text{applied}}$ by

$$\varepsilon_{\text{applied}} = \frac{L'_{\text{bridge}}-L_{\text{bridge}}}{L_{\text{bridge}}+L_{\text{island}}^0}. \quad (16)$$

The stretchability/compressibility characterizes how much the noncoplanar mesh design can accommodate further deformation. It is defined as the critical applied strain that leads to failure of interconnect or island, which occurs when the maximum strains in interconnect or island reach the corresponding failure strains $\varepsilon_{\text{bridge}}^{\text{failure}}$ and $\varepsilon_{\text{island}}^{\text{failure}}$ of the associated materials, respectively. The stretchability is determined by the condition at which the buckled interconnect returns to a flat state, at which point it cannot accommodate any additional stretching. This condition is obtained from $L'_{\text{bridge}}=L_{\text{bridge}}^0$ as

$$\varepsilon_{\text{stretchability}} = \frac{L_{\text{bridge}}^0-L_{\text{bridge}}}{L_{\text{bridge}}+L_{\text{island}}^0} = \frac{\varepsilon_{\text{pre}}}{1+(1+\varepsilon_{\text{pre}})\dfrac{L_{\text{island}}^0}{L_{\text{bridge}}^0}}. \quad (17)$$

The result clearly shows that long interconnects, short islands, and large prestrains increase the stretchability. For the limit of long interconnect $L_{\text{bridge}}^0 \gg L_{\text{island}}^0$, the stretchability is the prestrain ε_{pre}. For the other limit of short interconnect $L_{\text{bridge}}^0 \ll L_{\text{island}}^0$, the stretchability is $(L_{\text{bridge}}^0/L_{\text{island}}^0)[\varepsilon_{\text{pre}}/(1+\varepsilon_{\text{pre}})]$.

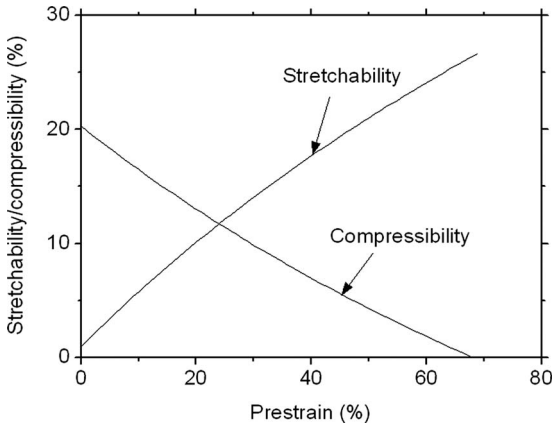

FIG. 6. Stretchability and compressibility vs the prestrain for the noncoplanar mesh design (island: 20×20 μm^2, 50 nm thick; interconnect: 20×4 μm^2, 50 nm thick) when the failure strains of interconnect and island are 1%.

The maximum strain in Eq. (9) for the interconnect now becomes $\varepsilon_{\text{bridge}}^{\max}=2\pi(h_{\text{bridge}}/L_{\text{bridge}}^0)\sqrt{(L_{\text{bridge}}^0-L'_{\text{bridge}})/L_{\text{bridge}}^0}$, while Eq. (12) still holds for the maximum strain in island. The compressibility is reached when they reach the corresponding failure strains $\varepsilon_{\text{bridge}}^{\text{failure}}$ and $\varepsilon_{\text{island}}^{\text{failure}}$, or when then neighbor islands start to contact. This gives the compressibility

$$\varepsilon_{\text{compressibility}} = \min\left[\frac{(1+\varepsilon_{\text{pre}})a^2-\varepsilon_{\text{pre}}}{1+(1+\varepsilon_{\text{pre}})\dfrac{L_{\text{island}}^0}{L_{\text{bridge}}^0}}, \frac{1}{1+(1+\varepsilon_{\text{pre}})\dfrac{L_{\text{island}}^0}{L_{\text{bridge}}^0}}\right], \quad (18)$$

where a is given in Eq. (15). For long interconnects (large a), the compressibility is $\varepsilon_{\text{compressibility}}=1/[1+(1+\varepsilon_{\text{pre}})\times(L_{\text{island}}^0/L_{\text{bridge}}^0)]$, corresponding to the contact of neighbor islands. For short interconnects (small a), the compressibility is $\varepsilon_{\text{compressibility}}=[(1+\varepsilon_{\text{pre}})a^2-\varepsilon_{\text{pre}}]/[1+(1+\varepsilon_{\text{pre}})\times(L_{\text{island}}^0/L_{\text{bridge}}^0)]$, corresponding to the failure of interconnect or island.

Figure 6 shows the stretchability and compressibility versus the prestrain for $L_{\text{island}}^0=20$ μm, $h_{\text{island}}=50$ nm, $L_{\text{bridge}}^0=20$ μm, $h_{\text{bridge}}=50$ nm, and $w_{\text{bridge}}=4$ μm. The failure strains of the interconnect and the island are assumed, for simplicity, to be $\varepsilon_{\text{bridge}}^{\text{failure}}=\varepsilon_{\text{island}}^{\text{failure}}=1\%$. The stretchability increases with the prestrain, but the compressibility decreases. Therefore, prestrain cannot be adjusted to give both maximum stretchability and maximum compressibility.

One way to achieve large stretchability and compressibility is to increase the length L_{bridge}^0 of interconnect. As shown in Fig. 7 for the same set of properties as Fig. 6 and the prestrain $\varepsilon_{\text{pre}}=50\%$, both stretchability and compressibility increase with the length of interconnect, though the compressibility increases much faster than the stretchability. The dot on the curve for compressibility separates the failure of interconnect or island (left of the dot) from the contact of neighbor islands (right of the dot).

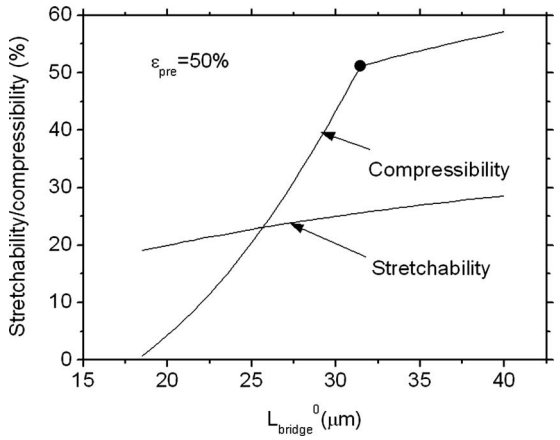

FIG. 7. Stretchability and compressibility vs the length of interconnect for the noncoplanar mesh design when the prestrain is 50%. The dot on the curve for compressibility separates the failure of interconnect or island (left of the dot) from the contact of neighbor islands (right of the dot).

V. CONCLUDING REMARKS

A mechanics model has been established for stretchable electronics with noncoplanar mesh designs. The results predict analytically the buckling amplitude, which agrees well with experiments (5.5% error) without any parameter fitting. The maximum strains in the interconnect and island are also obtained analytically, and are used to predict the stretchability and compressibility. The above model can be extended multilayer interconnects and islands by replacing the corresponding tension and bending rigidities.

ACKNOWLEDGMENTS

We thank for various helps of T. Banks in processing by use of facilities at Frederick Seitz Materials Research Laboratory. This materials is based on work supported by the National Science Foundation under Grant No. ECCS-0824129, NSFC, and the US Department of Energy, Division of Materials Sciences under Award No. DE-FG02-07ER46471, through the Materials Research Laboratory and Center for Microanalysis of Materials (Grant No. DE-FG02-07ER46453) at the University of Illinois at Urbana-Champaign. J.S. acknowledges the financial support from the College of Engineering at the University of Miami.

APPENDIX: ROTATION AT THE ENDS OF INTERCONNECTS

Section II assumes that interconnects are clamped, which gives vanishing rotation at the ends. The effect of nonvanishing rotation can be accounted for by the rotational springs with the spring constant k such that the bending moment M and the rotation θ at the ends of interconnects are related by $M=k\theta$. For each given M, the finite element analysis of islands and substrate in Sec. III gives the rotation θ, and the ratio M/θ gives the spring constant k. For example, $k=1.58\mu N$ for the elastic properties and thicknesses of islands and substrate in Fig. 5.

For an interconnect of length L_{bridge}^0 with rotational springs at its ends ($X=\pm L_{\text{bridge}}^0/2$), the equilibrium gives $EI(d^2w/dX^2)=-Nw+M$, where $EI=E_{\text{bridge}}h_{\text{bridge}}^3/12$ is the bending rigidity of the interconnect, w is the out-of-plane displacement that satisfies $w(-L_{\text{bridge}}^0/2)=w(L_{\text{bridge}}^0/2)=0$, N is the compressive force at the ends, and $M=kw'(-L_{\text{bridge}}^0/2)=-kw'(L_{\text{bridge}}^0/2)$ is the moment at the ends. The buckle profile is given by

$$w=A\frac{\cos\left(\frac{2\xi X}{L_{\text{bridge}}^0}\right)-\cos\xi}{1-\cos\xi}, \tag{A1}$$

where the amplitude A is to be determined, ξ is determined from $\tan\xi=-2EI/kL_{\text{bridge}}^0\xi$, and $\pi/2\le\xi\le\pi$. The limit $k\to\infty$ gives $\xi\to\pi$, and the buckle profile degenerates to Eq. (1) for a doubly clamped beam. The other limit $k\to0$ gives $\xi\to\pi/2$, and the buckle profile becomes $w=A\cos(\pi X/L_{\text{bridge}}^0)$, which satisfies $w=w''=0$ at two ends $X=\pm L_{\text{bridge}}^0/2$ of a simply supported beam.

The bending and membrane energies in interconnects are obtained from Eqs. (2) and (7), respectively. Minimization of total energy gives the amplitude

$$A=L_{\text{bridge}}^0\sqrt{\frac{2(1-\cos\xi)^2}{2\xi^2-\xi\sin(2\xi)}}\sqrt{\frac{L_{\text{bridge}}^0-L_{\text{bridge}}}{L_{\text{bridge}}^0}-\varepsilon_{\text{cr}}}, \tag{A2}$$

where $\varepsilon_{\text{cr}}=h_{\text{bridge}}^2/[3(L_{\text{bridge}}^0)^2][2\xi+\sin(2\xi)]\xi^2/[2\xi-\sin(2\xi)]$ is the critical buckling strain. The maximum compressive strain in the interconnect is the sum of membrane and bending strains, and it is given by

$$\begin{aligned}\varepsilon_{\text{bridge}}^{\max}&=\frac{2\xi h_{\text{bridge}}}{L_{\text{bridge}}^0}\sqrt{\frac{2\xi}{2\xi-\sin(2\xi)}}\sqrt{\frac{L_{\text{bridge}}^0-L_{\text{bridge}}}{L_{\text{bridge}}^0}-\varepsilon_{\text{cr}}}+\varepsilon_{\text{cr}}\\&\approx\frac{2\xi h_{\text{bridge}}}{L_{\text{bridge}}^0}\sqrt{\frac{2\xi}{2\xi-\sin(2\xi)}}\sqrt{\frac{L_{\text{bridge}}^0-L_{\text{bridge}}}{L_{\text{bridge}}^0}},\end{aligned} \tag{A3}$$

where the approximation holds for $(L_{\text{bridge}}^0-L_{\text{bridge}})/L_{\text{bridge}}^0\gg h_{\text{bridge}}/(L_{\text{bridge}}^0)^2$.

For $E_{\text{bridge}}=130$ GPa, $L_{\text{bridge}}^0=20$ μm, $h_{\text{bridge}}=50$ nm, and $L_{\text{bridge}}=17.5$ μm after relaxation, Eq. (A2) gives the amplitude $A=4.61$ μm, which agrees well with 4.50 μm given by Eq. (8). The maximum strain in the interconnect is 0.49% from Eq. (A3), which is smaller than 0.56% given by Eq. (11). Therefore, the rotation at the ends of interconnect can be neglected.

[1] G. P. Crawford, *Flexible Flat Panel Display Technology* (Wiley, New York, 2005).
[2] H. C. Ko, M. P. Stoykovich, J. Song, V. Malyarchuk, W. M. Choi, C.-J. Yu, J. B. Geddes, J. Xiao, S. Wang, Y. Huang, and J. A. Rogers, Nature (London) **454**, 748 (2008).
[3] V. Lumelsky, M. S. Shur, and S. Wagner, IEEE Sens. J. **1**, 41 (2001).
[4] T. Someya, T. Sekitani, S. Iba, Y. Kato, H. Kawaguchi, and T. Sakurai, Proc. Natl. Acad. Sci. U.S.A. **101**, 9966 (2004).
[5] A. Nathan, B. Park, A. Sazonov, S. Tao, I. Chan, P. Servati, K. Karim, T. Charania, D. Striakhilev, Q. Ma, and R. V. R. Mruthy, Microelectron. J. **31**, 883 (2000).
[6] S. P. Lacour, J. Jones, S. Wagner, T. Li, and Z. Suo, Proc. IEEE **93**, 1459 (2005).
[7] D. H. Kim, J. H. Ann, W. M. Choi, H. S. Kim, T. H. Kim, J. Song, Y. Huang, and J. A. Rogers, Science **320**, 507 (2008).

[8]D. H. Kim, J. Song, W. M. Choi, H. S. Kim, R. H. Kim, Z. J. Liu, Y. Huang, K. C. Hwang, Y. Zhang, and J. A. Rogers, Proc. Natl. Acad. Sci. U.S.A. **105**, 18675 (2008).
[9]S. P. Timoshenko and J. M. Gere, *Theory of Elastic Stability* (McGraw-Hill, New York, 1961).
[10]O. H. Nielsen, *Properties of Silicon* (INSPEC, IEE, London, 1988), p. 14.
[11]E. A. Wilder, S. Guo, S. Lin-Gibson, M. J. Fasolka, and C. M. Stafford, Macromolecules **39**, 4138 (2006).